Effect Of Nd Doping On The Phase Diagram Of $(Sm_{1-Y}nd_y)_{0.52}Sr_{0.48}mno_3$

Tamal Roy, Prosenjit Sarkar

Abstract: We have performed dc magnetization measurements on $(Sm_{1-y}Nd_y)_{0.52}Sr_{0.48}MnO_3$ ($0 \le y \le 1$) single crystals to study the nature of ferromagnetic to paramagnetic phase transition. For y = 0, ferromagnetic transition is first-order along with a discontinuous change in magnetization at T_C (110 K) with the presence of thermal hysteresis. With increasing Nd doping (y), T_C increases while thermal hysteresis starts to decrease which eventually vanishes at around y = 0.4, suggesting that first-order ferromagnetic transition becomes second-order in nature at that Nd concentration. The variation of T_C with y has been explained in terms of the average A-site cation radius and quenched disorder.

Index Terms: Ferromagnetic phase transition, hysteresis, manganite, narrowband system, phase diagram, quenched disorder, single crystal.

1 INTRODUCTION

Perovskite manganites $RE_{1-x}AE_x\ MnO_3$ (RE = rare earth ions, AE = alkaline earth ions) have extensively been studied due to their rich magnetoelectronic phase diagram, arising due to the close interplay between spin, charge, orbital and lattice degrees of freedom [1,2,3,4,5,6]. The effect of these competitive interactions becomes much stronger in case of narrow bandwidth systems. Other than bandwidth, quenched disorder (QD) also plays an important role on the nature of phase transition [3,4]. It has been observed that narrowband manganites with large QD show first-order ferromagnetic (FM) to paramagnetic (PM) phase transition whereas broadband manganites with high Curie temperature (T_C) undergoes conventional second-order FM-PM phase transition [5,6]. The band width of manganite systems can be controlled by tuning the average A-site cation radius, $\langle r_A \rangle$. In 1995, Hwang [7] and his workers have studied on the doped manganites with fixed carrier concentration and revealed a direct relationship between transition temperature T_C and $\langle r_A \rangle$. With the increase of $\langle r_A \rangle$, T_C was observed to increase up to a certain value, but above that, T_C starts to decrease. At that time, the anomalous nature of T_C was not clear but they argued that this may be due to the increased size mismatch between RE^{3+} and AE^{2+} ions. In 1996, Rodriguez-Martinez and Attfield [8] have shown that T_C can be reduced by a large factor by increasing the size mismatch between RE^{3+} and AE^{2+} cations, keeping $\langle r_A \rangle$ constant. The size mismatch of A-site cations in the doped manganites is generally called QD, whose magnitude can be calculated from the variance in the ionic radii [8]

$$\sigma^2 = \langle r_A^2 \rangle - \langle r_A \rangle^2 = \sum x_i r_i^2 - (\sum x_i r_i)^2, \quad (1)$$

where x_i and r_i are the fractional occupancies and effective ionic radii of cations.From the electronic phase diagram [9] of various $RE_{1-x}AE_xMnO_3$ (x = 0.45) crystals in the plane of $\langle r_A \rangle$ vs. σ^2, it is clear RE = Sm with AE = Sr system can be considered as a narrowband manganite with relatively large QD. In this paper, we present the nature of FM-PM phase transition in $(Sm_{1-y}Nd_y)_{0.52}Sr_{0.48}MnO_3$ ($0 \le y \le 1$). We have shown from the magnetization (M) studies that FM-PM transition for y = 0 is first-order at T_C = 110 K. With increasing Nd concentration y, T_C increases, whereas the thermal hysteresis width in magnetization decreases that eventually vanishes at around y = 0.4, suggesting that y = 0.4 is a critical concentration at which first-order FM-PM transition becomes second-order in nature.

2 EXPERIMENTAL DETAILS

In order to understand the physical phenomena, samples for measurement have to be prepared. On the basis of regularity pattern, the samples can be put into two broad categories: the single crystal and the polycrystal. A single crystal is a crystalline solid in which the crystal lattice of the entire sample is continuous and unbroken to the edges of the sample, with no grain boundaries. On the other hand, polycrystal consists of a large number of crystallites of various shapes and sizes packed to one another in a quite irregular way along the interfaces. For the experimental study of different physical properties of a system, it is crucial to obtain good quality single crystals of the material concerned, since for polycrystalline materials, the properties of the grain boundaries often manifest themselves stronger than the properties of the material itself. Polycrystalline samples of $(Sm_{1-y}Nd_y)_{0.52}Sr_{0.48}MnO_3$ ($0 \le y \le 1$) were prepared by conventional solid state reaction technique. The starting materials, Sm_2O_3, Nd_2O_3, $SrCO_3$, and Mn_3O_4 were weighted in stoichiometric ratio and were ground thoroughly in an agate mortar by using ethanol. The mixture was put in a platinum crucible and calcined in air at around 1100 ^{0}C for 1 day. We have used a tube furnace that can be operated in programme mode, which is useful to set a particular temperature for required hours. Also the rate of heating or cooling can be operated in programme mode. The obtained powder was pulverized and again sintered in the same condition to ensure its homogeneity. The polycrystalline powder, prepared by solid state reaction technique was formed to cylindrical shape with ~5 mm in diameter and ~10 cm length with the use of hydrostatic pressure of 5 ton and fired at 1350◦C for 20 hours

- *Tamal Roy is currently working as Assistant Teacher in Santinagar High School, Barrackpore, Kolkata – 700122, India. E-mail: tamalroy232@gmail.com*
- *Prosenjit Sarkar is currently working as Assistant Professor in Department of Physics, Serampore College, Serampore – 712201, India. E-mail: psphysics1981@gmail.com (Corresponding Author)*

in air. Then, the rod was divided into two pieces and fitted into the upper and lower shaft of floating zone image furnace as feed and seed rod, respectively. The feed and seed rods were moved down and upward respectively until they touched with each other. A suitable voltage was applied to the lamps of floating zone image furnace, so that the produced heat can melt the junction region of the rods and form a molten zone that is maintained between two rods of the solid without any container. The molten part stabilizes due to the balance between surface tension force and gravitational force. Then the feed and seed rods were rotated in the opposite direction at the rate of 25 rpm. By moving the molten zone slowly downward with the growth rate of 8-10 mm/h, a single crystal can be grown. The growth takes place inside a quartz tube at oxygen atmosphere. Thus, we prepared the single crystals of $(Sm_{1-y}Nd_y)_{0.52}Sr_{0.48}MnO_3$ for $0 \leq y \leq 1$

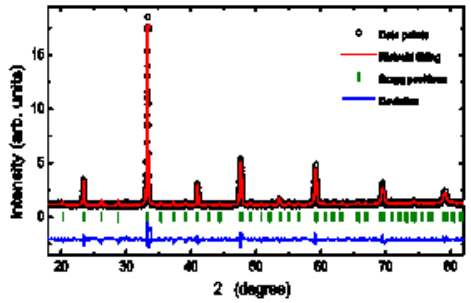

Fig. 1. *X-ray powder diffraction (XRD) pattern of Sm0.52Sr0.48MnO3 at room temperature. The red line corresponds to the Rietveld refinement of the diffraction pattern with space group Pbnm.*

The qualities of the crystals were carefully checked by different techniques like x-ray powder diffraction (XRD), Laue diffraction etc. Samples for powder XRD were prepared by grinding the samples and pressed on a glass holder to achieve a smooth flat surface. We have measured the diffraction data using the diffractometer in reflection mode. Using a automated goniometer, step by step scattered intensity has been measured. Figure 1 shows the XRD pattern for $Sm_{0.52}Sr_{0.48}MnO_3$ at room temperature. The diffraction patterns for various compositions show that all the samples have a perovskite orthorhombic structure with Pbnm space group. The lattice parameters obtained from the Rietveld refinements for y = 0 sample are a = 5.4414 Å, b = 5.4176 Å, and c = 7.6521 Å, which are comparable with those reported by Tomioka et. al. [10]

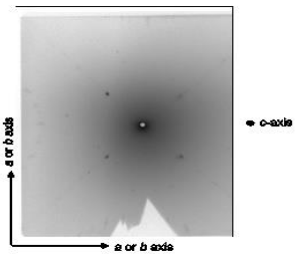

Fig. 2. *Laue pattern of Sm0.52Sr0.48MnO3 at room temperature.*

In powder XRD, a finely powered specimen is placed in monochromatic beam of x-rays, whereas in Laue method, a single crystal specimen is held stationary in a beam of x-rays of continuous wavelength. Each set of crystal planes chooses its own wavelength from the incident beam and satisfies the Bragg's law of diffraction. The diffraction pattern consists of a series of spots, which is basically a map of reciprocal lattice of the crystal under experiment. As the symmetry properties of reciprocal lattice are directly related to the symmetry properties of the direct lattice, the pattern must show the symmetry of the crystal in the used orientation. Thus the Laue pattern is convenient for checking the orientation of the crystals. There are two types of Laue method such as transmission method and back reflection method. In transmission method, the diffracting crystal lies between the source and the recording screen, where as screen is located between the source and the crystal in case of back reflection technique, in which x-ray passes the screen through a pin-hole arrangement, reaches to crystal, diffracts, and then produces a series of spots on the screen. The crystal orientation is determined from the position of the spots by indexing them using Greninger chart. The parent compound, $Sm_{0.52}Sr_{0.48}MnO_3$ crystal was oriented using Laue back reflection method which is shown in Figure 2. The dc magnetization measurements were done with the help of a superconducting quantum interference device magnetometer (MPMS, Quantum design) over a wide range of temperature. External magnetic field (H) was applied along the longest sample direction and the data were corrected for the demagnetization effect.

3 RESULTS AND DISCUSSION

Figure 3 shows the temperature dependence of magnetization of $(Sm_{1-y}Nd_y)_{0.52}Sr_{0.48}MnO_3$ single crystal for different Nd

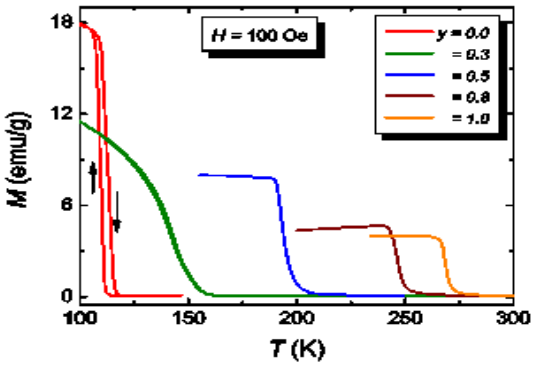

Fig. 3. *Temperature (T) dependence of magnetization (M) of (Sm1-yNdy)0.52Sr0.48MnO3 (0 ≤ y ≤ 1) single crystals measured at 100 Oe external magnetic field. The arrows indicate the heatinf and cooling cycles.*

concentration y. For y = 0, M exhibits a sharp drop at T_C = 110 K along with thermal hysteresis of width, $\Delta T \sim 4$ K, indicating that FM to PM phase transition is first-order in nature. The transition temperature T_C is determined from the minimum of (dM/dT) vs. T curve. With increasing Nd doping, both magnetization as well as the sharpness of M(T) curve decrease, whereas T_C shifts towards the higher temperature as shown in Figure 4 (a). The width of the thermal hysteresis

in magnetization starts to decrease with increasing y and vanishes above y ~ 0.4 [Figure 4 (a)]. This indicates that first-order nature of FM transition gets weakened with Nd doping and becomes second-order at around y = 0.4. The variation of T_C with y can be explained by considering the average A-site cation size, $\langle r_A \rangle$ and A-site cation disorder, σ^2. Rodriguez-Martinez and Attfield have studied the effect of $\langle r_A \rangle$ and σ^2 on the FM-metal to PM-insulator transition temperature of $RE_{0.7}AE_{0.3}MnO_3$ perovskites

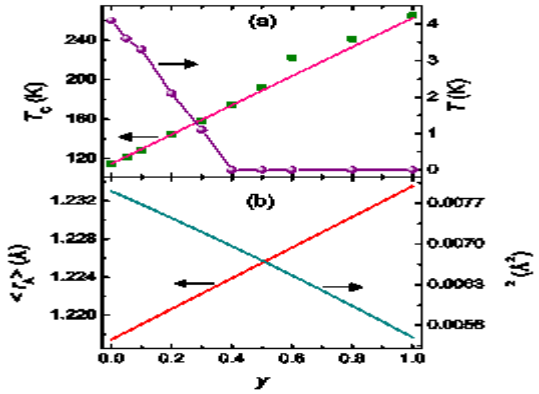

Fig. 4. *(a) Ferromagnetic to paramagnetic transition temperature (TC) and thermal hysteresis width (ΔT) of (Sm1-yNdy)0.52Sr0.48MnO3 (0 ≤ y ≤ 1) single crystals as a function of Nd concentration (y). (b) y dependence of average A-site cation radius (<rA>) and quenched disorder (σ2).*

by using various RE (La, Pr, Nd, Sm) and AE (Ca, Sr, Ba) ions and their results show that T_C can be expressed as [8]

$$T_C(\langle r_A \rangle, \sigma^2) = T_C(r^0_A, 0) - P_2 [r^0_A - \langle r_A \rangle]^2 - P_1 [\sigma^2], \quad (2)$$

where r^0_A is the ideal radius for an undistorted cubic perovskite and $T_C(r^0_A, 0)$ is an estimate of the transition temperature for an ideal ($\langle r_A \rangle = r^0_A$), disorder-free ($\sigma^2 = 0$) system. As both $\langle r_A \rangle$ and σ^2 of $(Sm_{1-y}Nd_y)_{0.52}Sr_{0.48}MnO_3$ depend on y, T_C can be expressed as a function of y as [8]

$$T_C(y) = T_C(r^0_A, 0) - P_2 [r^0_A - \langle r_A \rangle(y)]^2 - P_1 [\sigma^2(y)], \quad (3)$$

Standard ionic radii (ninefold coordination) with values 1.132, 1.163, and 1.31 Å for Sm^{3+}, Nd^{3+}, and Sr^{2+}, respectively, are used to calculate $\langle r_A \rangle$ and σ^2 [equation (1)] for different values of y. With increasing y, $\langle r_A \rangle$ increases while σ^2 decreases [as shown in Figure 4 (b)] and according to the above equation, both of these changes enhance the T_C. Following equation (3), we try to fit our experimentally measured T_C for different y and find that the fitting is excellent with $T_C(r^0_A, 0) = 520 \pm 14$ K, $P_2 = 37000 \pm 1200$ K/Å^2, $P_1 = 33000 \pm 1000$ K/Å^2.

4 CONCLUSION

In conclusion, we present the nature of ferromagnetic to paramagnetic phase transition in $(Sm_{1-y}Nd_y)_{0.52}Sr_{0.48}MnO_3$ ($0 \leq y \leq 1$). From dc magnetization studies, we have shown that ferromagnetic to paramagnetic phase transition for y = 0 is first-order at T_C = 110 K. With increasing Nd concentration y, T_C increases, whereas the thermal hysteresis width in magnetization decreases that eventually vanishes at around y = 0.4, suggesting that y = 0.4 is a critical concentration at which first-order ferromagnetic transition becomes second-order in nature. The phase diagram T_C vs. y can be addressed by considering the average A-site cation radius and quenched disorder.

5 ACKNOWLEDGMENT

The authors would like to acknowledge Prof. P. Mandal for his help to prepare the samples and to collect the experimental data.

6 REFERENCES

[1] C. N. R. Rao and B. Raveau, “Colossal Magnetoresistance, Charge Ordering and Related Properties of Manganese Oxides”, World Scientific, Singapore, 1998.

[2] M. B. Salamon and M. Jaime, “The physics of manganites: Structure and transport,” Rev. Mod. Phys. vol. 73, pp. 583, 2001.

[3] E. Dagotto, T. Hotta, and A. Moreo, “Colossal magnetoresistant materials: the key role of phase separation,” Phys. Rep. Vol. 344, pp. 1, 2001.

[4] E. Dagotto, “Complexity in Strongly Correlated Electronic Systems,” vol. 309, pp. 257, 2005.

[5] Y. Tokura, “Critical features of colossal magnetoresistive manganites,” vol. 69, pp. 797, 2006.

[6] P. K. Siwach, H. K. Singh and O. N. Srivastava, “Low field magnetotransport in manganites,” J. Phys.: Condens. Matter, vol. 20, pp. 273201, 2008.

[7] H. Y. Hwang, T. T. M. Palstra, S. W. Cheong, and B. Batlogg, “Pressure effects on magnetoresistance in doped manganese perovskites,” Phys. Rev. B, vol. 52, pp. 15046, 1995.

[8] L. M. Rodriguez-Martinez and J. P. Attfield, “Cation disorder and size effects in magnetoresistive manganese oxide perovskites,” Phys. Rev. B, vol. 54, pp. R15622, 1996.

[9] Y. Tomioka and Y. Tokura, “Global phase diagram of perovskite manganites in the plane of quenched disorder versus one-electron bandwidth,” Phys. Rev. B, vol. 70, pp. 014432, 2004.

[10] Y. Tomioka, H. Hiraka, Y. Endoh, and Y. Tokura, “Multicritical phase diagram of the electronic states in $Sm_{1-x}Sr_xMnO_3$ ($0.3 < x < 0.6$) single crystals with controlled carrier density,” Phys. Rev. B, vol. 74, pp. 104420, 2006.